Electrochemical and Solid-State Letters, **14** (2) C5-C7 (2011)
1099-0062/2010/14(2)/C5/3/$28.00 © The Electrochemical Society

Electrochemical Properties of Intermetallic Phases and Common Impurity Elements in Magnesium Alloys

A. D. Südholz,[a,*] N. T. Kirkland,[b] R. G. Buchheit,[c,] and N. Birbilis[a,***,z]**

[a]*ARC Center of Excellence for Design in Light Metals, Department of Materials Engineering, Monash University, 3800 Victoria, Australia*
[b]*Department of Mechanical Engineering, University of Canterbury, Christchurch 8041, New Zealand*
[c]*Fontana Corrosion Center, Department of Materials Science and Engineering, The Ohio State University, Columbus, Ohio 43210, USA*

The electrochemical properties of the key intermetallic particles that form in commercial Mg alloys are presented. Results were collected via microcapillary electrochemical testing upon bulk intermetallic analogs in dilute chloride solution. The intermetallics investigated were $Mg_{17}Al_{12}$, Mg_2Al_3, Mg_2Ca, $Mg_{12}Ce$, $Mg_{12}La$, Mg_3Nd, Mg_2Si, $Mg_{24}Y_5$, and $MgZn_2$. It was found that the intermetallic phases, with the exception of Mg_2Ca, were more noble than Mg, supporting increased levels of cathodic kinetics; however, the variation in electrochemical response between intermetallics was large in terms of corrosion potential, presence of a passive window, and currents sustained over a range of potentials.
 [DOI: 10.1149/1.3523229]

Manuscript submitted September 9, 2010; revised manuscript received November 1, 2010. Published December 6, 2010.

Magnesium (Mg) alloys possess good specific strength and casting properties; however, their more widespread commercial application has been severely limited by their relatively poor resistance to corrosion.[1-3] Unlike other alloys (i.e., those based on Al or Fe), Mg alloys are incapable of sustaining a protective passive film and subsequently suffer from continued dissolution in neutral chloride environments,[4-6] including atmospheric exposure. The limited solubility of most elements in Mg results in the formation of Mg containing intermetallic particles (IMPs). As a consequence, the investigation of the corrosion behavior of Mg alloys requires a focus on the link between microstructural features and their impact on the corrosion reaction kinetics.

Common (commercial) Mg alloys present IMPs from typical alloying additions of Al, Zn, rare earths (Ce, La, Nd), Y, Ca, and Si. The IMPs typically formed include $Mg_{17}Al_{12}$, Mg_2Ca, $Mg_{12}Ce$, $Mg_{12}La$, Mg_3Nd, Mg_2Si, $Mg_{24}Y_5$, Mg_3Al_2, and $MgZn_2$, respectively.[1-3,7]

This study reports the electrochemical properties of the above intermetallics in a consolidated presentation and, for several IMPs, revealing such properties for the first time. The interpretation of the electrochemical response of intermetallics has been identified as critical to Mg alloys for over 20 years commencing with the work of Lunder et al.[8] and conversely has led to major developments in the understanding of corrosion of Al alloys.[9-11] In spite of this, a detailed holistic study has not emerged until now. The test electrolyte is investigated herein in 0.1 M NaCl because it is a simple approximation to atmospheric conditions and allows data to be compared with the large amount of data on commercial Mg alloys in the literature. The aim of this work is to elucidate the individual electrochemical behavior of each intermetallic phase in order to contribute to an improved universal understanding of the corrosion of Mg alloys. Because IMPs exist on a small size range ($\sim < 20$ μm diameter) in commercial alloys, the investigation of their electrochemical properties necessitates the preparation of such IMPs in a more bulk form. Consequently, the IMPs tested herein were created by casting ingots to contain a population of the target IMPs on the size scale of >100 μm diameter (the approach for this is detailed in Ref. 10). Microcapillary electrochemical testing allows for electrochemical interrogation of features at this length scale and is thus the approach pursued herein for determining the intermetallic electrochemistry uniquely.

Additionally, we present the relevant polarization data for a number of pure elements that are typically designated as "impurities" in Mg, because their respective solubility is so low that such elements form particles of the respective pure metal in the Mg matrix,[12,13] (i.e., pure Fe exists as a particle in Mg, as it is insoluble).

Experimental

Materials.— The feedstock materials used in the preparation of all the alloys tested in this study were nominally of at least 99.99% purity, and metals were supplied by Alfa Aesar. Table I lists the intermetallic phases investigated in this study and details the corresponding production method, characterization technique, and reference of characterization work where relevant. In all cases, the intermetallics were quantitatively characterized by the combination of chemistry (X-ray) and structure (diffraction) to ensure that the target IMP was achieved. Pure metals typically present as impurity elements were also investigated in this study, and such metals were of commercial purity: Copper (Cu), iron (Fe), manganese (Mn), and nickel (Ni).

Sample preparation.— The sample surface to be exposed to the electrolyte was ground using a SiC paper to a 2400 grit finish to achieve a uniformly smooth surface and to allow the optical identification of intermetallic sites as a precursor to microelectrochemical cell testing. Cleaning after grinding steps was done using ethanol (to avoid reaction with water) and specimens were subsequently dried under argon (Ar) gas prior to electrochemical analysis.

Electrochemical analysis.— The electrochemical testing of intermetallic particles was carried out using a microcapillary electrochemical cell method,[16] of the configuration as previously described in Ref. 10 and reviewed in Ref. 17. This technique defines the working electrode area by the area of sample that comes into contact with the opening of a microcapillary filled with the electrolyte. The electrolyte is in contact with a small-wire counter electrode and a saturated calomel reference electrode. The capillary opening in this work was nominally ~80 μm in diameter and will vary with each capillary—with the size being sufficiently small to individually isolate intermetallic particles. In this instance, potentiodynamic polarization curves were executed at 10 mV/s from 100 mV more negative than the open circuit and scanned until either a breakdown was exceeded or the current density recorded exceeded 1 mA/cm^2. It was found that the results in such instances correlated with the individual anodic and cathodic scans, so it was decided that given the intricate nature of the test, a standardized single sweep should be adopted.

In the case where bulk metals were tested, an electrochemical "flat-cell" was used, with a working electrode area of 1 cm^2. Each sample was tested in quiescent 0.1 M NaCl, using a Bio-Logic VMP 3Z potentiostat under the control of EC-LAB software.

* Electrochemical Society Student Member.
** Electrochemical Society Fellow.
*** Electrochemical Society Active Member.
z E-mail: nick.birbilis@monash.edu

Table I. Intermetallic phases present in common Mg alloy systems with the corresponding sample production method and characterization.

Alloy system	Intermetallic	Production method	Characterization[a]	Reference
Mg–Al	$Mg_{17}Al_{12}$	Induction melting	EBSD	—
Al–Mg	Mg_2Al_3	Induction melting	EBSD	10
Mg–Ca	Mg_2Ca	High pressure die cast	EBSD	14
Mg–Ce	$Mg_{12}Ce$	High pressure die cast	TEM	15
Mg–La	$Mg_{12}La$	High pressure die cast	TEM	15
Mg–Nd	Mg_3Nd	High pressure die cast	TEM	15
Mg–Si	Mg_2Si	Arc melting	EBSD	10
Mg–Y	$Mg_{24}Y_5$	Induction melting	EBSD	—
Mg–Zn	$MgZn_2$	Induction melting	EBSD	10

[a] EBSD, electron backscatter diffraction; TEM, transmission electron microscopy.

Results

Potentiodynamic polarization was performed on each intermetallic phase at least five times and the average corresponding curves are displayed in Fig. 1. It should be mentioned that no specific effort was made to control the oxygen concentration in such tests, because the contribution of oxygen is negligible where the dominant cathodic reaction is water reduction (not oxygen reduction) while the anodic branch is independent of the oxygen concentration.

The cathodic polarization curves of each of the pure metals that nominally form impurity elements are displayed in Fig. 2. These curves were included in this study to provide a holistic representation of the potential electrochemical heterogeneity that can exist in Mg alloys. Additionally, the average E_{corr} values extracted from the aforementioned potentiodynamic polarization (PDP) curves are detailed in Table II.

Discussion

Polarization behavior of Mg-based IMPs.— From the observation of the PDP curves of each of these intermetallic phases (Fig. 1), it can be seen that the E_{corr} for each of the IMPs varies by a significant amount. This is reflective of both the reactivity of the alloying element that combines with Mg and the stoichiometric ratio of this combination.

Table II also presents the values of E_{corr}; however, it is also visually obvious from Fig. 1 that in all cases, with the exception of Mg_2Ca, IMPs display a E_{corr} nobler than that of pure Mg.

General observations from Fig. 1 are as follows:

- The relative increase in E_{corr} of the IMPs with respect to Mg reflects the electrochemistry of the respective alloying element.
- Al, Ce, La, Nd, and Si containing IMPs were "spontaneously passive," indicating that they display some electrochemical stability/passivity in 0.1 M NaCl, albeit the passive current densities measured are in the range up to 10 $\mu A/cm^2$.
- The electrochemical effect of rare-earth elements is not the same. There are significant differences between Ce, La, and Nd containing intermetallics. The relative nobility scales as $Mg_{12}Ce$, Mg_3Nd, and $Mg_{12}La$. The relative cathodic efficiency scales as $Mg_{12}Ce$, $Mg_{12}La$, and Mg_3Nd. Consequently, $Mg_{12}Ce$ would result in most corrosion of the Mg.
- Y (strictly a rare earth but not one of the lanthanide elements) behaves vastly different to Ce, La, and Nd. The intermetallic $Mg_{24}Y_5$ sustains higher anodic and cathodic reaction kinetics than does Mg while only slightly more noble than does Mg. This relative nobility, however, is minor, and it is expected (and observed) that when Mg is alloyed with Y, corrosion rates accelerate.[18]

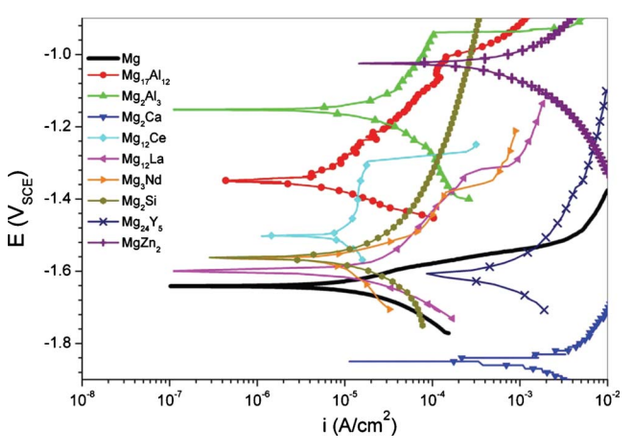

Figure 1. (Color online) Potentiodynamic polarization traces of each intermetallic phase present in the binary Mg alloys along with pure Mg for comparison, in 0.1 M NaCl.

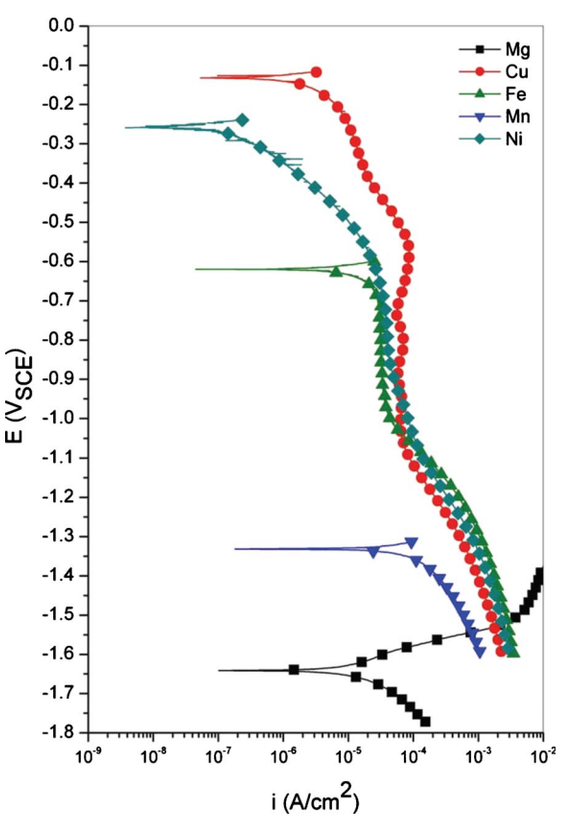

Figure 2. (Color online) Potentiodynamic polarization traces of each impurity element along with pure Mg for comparison, in 0.1 M NaCl.

Table II. Corrosion potentials (E_{corr}) for intermetallic phases and pure metals in 0.1 M NaCl.

Alloy system	Intermetallic	Corrosion potential (V_{SCE})
Mg–Ca	Mg_2Ca	−1.75
Mg	—	−1.65
Mg–Y	$Mg_{24}Y_5$	−1.60
Mg–La	$Mg_{12}La$	−1.60
Mg–Nd	Mg_3Nd	−1.55
Mg–Si	Mg_2Si	−1.54
Mg–Ce	$Mg_{12}Ce$	−1.50
Mg–Al	$Mg_{17}Al_{12}$	−1.35
Mn	—	−1.28
Mg–Zn	$MgZn_2$	−1.03
Al–Mg	Mg_2Al_3	−1.01
Fe	—	−0.60
Ni	—	−0.22
Cu	—	−0.15

• Al is efficient at ennobling the IMP. The result of this is that the ultimate intersection between Mg and the Al containing IMP occurs at high rates.

• In essentially all cases, the IMPs are able to support higher rates of reduction reaction kinetics compared to pure Mg, which correlates elegantly with the low exchange current density for water reduction of pure Mg,[19] which is one of the lowest values. Consequently, in general, IMPs serve as efficient local cathodes in Mg.

• $MgZn_2$, while more noble than Mg, is not spontaneously passive. This IMP supports rather high rates of reduction reaction owing to greater cathodic efficiency of Zn with respect to Mg.

• Ca is electrochemically active, and the intermetallic Mg_2Ca undergoes dissolution at tremendously high rates. It can dissolve in preference to Mg, and indeed Mg–Ca alloys have the highest corrosion rates of essentially any candidates for structural metals.[14] This point, and that above, make the development of biodegradable Mg alloys a major challenge, because Zn and Ca are very biocompatible but electrochemically quite reactive.

Revealing the above information was only possible via microelectrochemical testing, even in this specific case where intermetallic analogs were cast (because large defect-free casting of intermetallics is not readily possible). Bearing in mind any caveats associated with microelectrochemical testing,[17] the above information sheds significant light on the behavior of commercial Mg alloys and mechanistic aspects that dictate the morphology and extent of localized corrosion that evolves upon such alloys.

Rather than spending significant effort discussing the electrochemical results here in the context of examples relevant to the authors themselves, it is considered much more valuable to allow the raw data in Fig. 1 to be available[20] such that the data can be used by others wishing to analyze their alloys/systems and those wishing to develop predictive models such as those in Ref. 21.

Polarization behavior of the metals forming insoluble impurity particles in Mg alloys.— The hexagonal (hexagonal closed-packed) structure combined with the relatively small atomic radius of Mg results in low levels of solid solubility of other elements.[1-3] As a consequence, there exist a limited number of soluble elements which can be alloyed with Mg. Insoluble elements remain in the Mg matrix in pure metallic form and are the cause of significant deterioration in corrosion resistance of Mg alloys. In order to reveal the severity of this effect, Fig. 2 reveals the relevant portions of the polarization curves for pure metals. Each of the pure metals has a corrosion potential that is more noble than pure Mg. The cathodic branch of each respective PDP curve has been recorded down to the corrosion potential of Mg to demonstrate the intersection point of the two coupled. In the case of Ni, Cu, and Fe, the intersection point corresponds to a current density in excess of about 2 orders of magnitude higher than the corrosion current density of Mg. This phenomenon renders Mg highly susceptible to rapid corrosion in the presence of such impurities. This is in contrast to the coupling of Mg with Mg containing intermetallics, which have only moderate by coupled currents when compared to pure metals (because the intermetallics include some fraction of Mg in their structure). In the case of Mn, we see a lower corrosion potential and slightly lower cathodic kinetics sustained upon Mn with respect to Cu/Fe/Ni. This would suggest that Mn may not be as deleterious, particularly in alloys where the potential of the base alloy is ennobled by other elements—and is found to empirically be the case, given low levels of Mn are added to alloys such as AM60 for the development of mechanical properties (albeit at the expense of corrosion resistance).

Conclusions

Careful alloy casting and sample preparation made it possible to produce specimens amenable to microelectrochemical testing (i.e., with a population of the desired intermetallic particles existing in the size range of >100 μm). As such, the electrochemical properties of Mg-based intermetallic phases were investigated and reported—many for the very first time. These phases that play a significant role in the localized corrosion behavior of Mg alloys were found to be cathodic to Mg, with the exception of Mg_2Ca. Intermetallics were found to support reduction reactions at greater rates than Mg, with variations in the electrochemical response allowing for discrimination between the relative behavior of the intermetallics studied with regard to corrosion risk. The information herein can be used to develop damage models for Mg alloys and may be integrated into alloy design—serving as key information to the Mg corrosion community.

Acknowledgments

The Australian Research Council's Centre of Excellence for Design in Light Metals and the DIIRD-funded Victorian Facility for Light Metals Surface Technology are gratefully acknowledged. Thanks are extended to the CAST Co-operative Research Centre for the preparation of Mg-RE specimens.

Monash University assisted in meeting the publication costs of this article.

References

1. K. U. Kainer, *Magnesium—Alloys and Technology*, Wiley VCH-Verlag, Weinheim (2003).
2. I. J. Polmear, *Light Alloys*, 3rd ed., Arnold, London (1995).
3. W. Unsworth and J. F. King, *Magnesium Technology*, Institute of Metals, London (1986).
4. R. Tunold, H. Holtan, M.-B. H. Berge, A. Lasson, and R. Steen-Hansen, *Corros. Sci.*, **17**, 353 (1977).
5. G. L. Makar and J. Kruger, *Int. Mater. Rev.*, **38**, 138 (1993).
6. E. Ghali, W. Dietzel, and K. U. Kainer, *J. Mater. Eng. Perform.*, **13**, 7 (2004).
7. L. L. Rokhlin, *Magnesium Alloys Containing Rare Earth Metals*, Taylor & Francis, London (2003).
8. O. Lunder, J. Lein, T. K. Aune, and K. Nisancioglu, *Corrosion*, **45**, 741 (1989).
9. R. G. Buchheit, *J. Electrochem. Soc.*, **142**, 3994 (1995).
10. N. Birbilis and R. G. Buchheit, *J. Electrochem. Soc.*, **152**, B140 (2005).
11. N. Birbilis and R. G. Buchheit, *J. Electrochem. Soc.*, **155**, C117 (2008).
12. S. J. Splinter, N. S. McIntyre, P. A. W. van der Heide, and T. Do, *Surf. Sci.*, **317**, 194 (1994).
13. J. A. Boyer, *The Corrosion of Magnesium and of the Magnesium Alloys Containing Manganese*, American Magnesium Corporation, Pittsburgh, PA (1927).
14. N. T. Kirkland, N. Birbilis, J. Walker, T. B. Woodfield, G. J. Dias, and M. P. Staiger, *J. Biomed. Mater. Res., Part B: Appl. Biomater.*, **95B**, 91 (2010).
15. N. Birbilis, M. A. Easton, A. D. Sudholz, S. M. Zhu, and M. A. Gibson, *Corros. Sci.*, **51**, 683 (2009).
16. T. Suter and H. Böhni, *Electrochim. Acta*, **43**, 2843 (1998).
17. N. Birbilis, B. N. Padgett, and R. G. Buchheit, *Electrochim. Acta*, **50**, 3536 (2005).
18. M. Liu, P. Schmutz, P. J. Uggowitzer, G. Song, and A. Atrens, *Corros. Sci.*, **52**, 3687 (2010).
19. J. O'M. Bockris, A. K. N. Reddy, and M. E. Gamboa-Aldeco, *Modern Electrochemistry*, Chap. 10, Kluwer, New York (2000).
20. http://users.monash.edu.au/~nickbir/AIPdata.xls, last accessed December 3, 2010.
21. M. K. Cavanaugh, R. G. Buchheit, and N. Birbilis, *Eng. Fract. Mech.*, **76**, 641 (2009).